

Measuring permeability of porous materials at low frequency range via acoustic transmitted waves

Z. E. A Fellah, M. Fellah, F. G. Mitri, N. Sebaa, C. Depollier, and W. Lauriks

Citation: [Review of Scientific Instruments](#) **78**, 114902 (2007); doi: 10.1063/1.2804127

View online: <http://dx.doi.org/10.1063/1.2804127>

View Table of Contents: <http://scitation.aip.org/content/aip/journal/rsi/78/11?ver=pdfcov>

Published by the [AIP Publishing](#)

Articles you may be interested in

[Acoustical properties of air-saturated porous material with periodically distributed dead-end pores](#)

J. Acoust. Soc. Am. **137**, 1772 (2015); 10.1121/1.4916712

[Transient acoustic wave propagation in air-saturated porous media at low frequencies](#)

J. Appl. Phys. **102**, 084906 (2007); 10.1063/1.2798930

[Measuring flow resistivity of porous materials at low frequencies range via acoustic transmitted waves](#)

J. Acoust. Soc. Am. **119**, 1926 (2006); 10.1121/1.2179749

[A time-domain model of transient acoustic wave propagation in double-layered porous media](#)

J. Acoust. Soc. Am. **118**, 661 (2005); 10.1121/1.1953247

[Acoustical characterization of absorbing porous materials through transmission measurements in a free field](#)

J. Acoust. Soc. Am. **102**, 1982 (1997); 10.1121/1.419689



OXFORD
INSTRUMENTS
The Business of Science®

**'On the way to a
graphene spin field effect transistor'**
by Prof. Barbaros and the Özyilmaz Group at National University of Singapore

Download a FREE application note

Measuring permeability of porous materials at low frequency range via acoustic transmitted waves

Z. E. A Fellah

Laboratoire de Mécanique et d'Acoustique, CNRS-UPR 7051, 31 Chemin Joseph Aiguier, Marseille 13009, France

M. Fellah

Laboratoire de Physique Théorique, Faculté de Physique, USTHB, BP 32 El Alia, Bab Ezzouar 16111, Algeria

F. G. Mitri

Mayo Clinic and Foundation, Department of Physiology and Biomedical Engineering, Ultrasound Research Laboratory, 200 First Street SW, Rochester, Minnesota 55905, USA

N. Sebaa

Laboratorium voor Akoestiek en Thermische Fysica, Katholieke Universiteit Leuven, Celestijnenlaan 200 D, B-3001 Heverlee, Belgium

C. Depollier

Laboratoire d'Acoustique de l'Université du Maine, UMR-CNRS 6613, Université du Maine, Avenue Olivier Messiaen, 72085 Le Mans Cedex 09, France

W. Lauriks

Laboratorium voor Akoestiek en Thermische Fysica, Katholieke Universiteit Leuven, Celestijnenlaan 200 D, B-3001 Heverlee, Belgium

(Received 4 April 2007; accepted 6 October 2007; published online 28 November 2007)

An acoustical transmission method is proposed for measuring permeability of porous materials having rigid frame. Permeability is one of the several parameters required by acoustical theory to characterize porous materials such as plastic foams and fibrous or granular materials. The proposed method is based on a temporal model of the direct and inverse scattering problem for the diffusion of transient low frequency waves in a homogeneous isotropic slab of porous material having a rigid frame. This time domain model of wave propagation was initially introduced by the authors [Z.E.A Fellah and C. Depollier, *J. Acoust. Soc. Am.* **107**, 683 (2000)]. The viscous losses of the medium are described by the model devised by Johnson *et al.* [*J. Fluid. Mech.* **176**, 379 (1987)]. Reflection and transmission scattering operators for a slab of porous material are derived from the responses of the medium to an incident acoustic pulse. The permeability is determined from the expressions of these operators. Experimental and numerical validation results of this method are presented. This method has the advantage of being simple, rapid, and efficient. © 2007 American Institute of Physics.

[DOI: [10.1063/1.2804127](https://doi.org/10.1063/1.2804127)]

I. INTRODUCTION

The acoustic characterization of porous materials saturated by air¹⁻⁴ such as plastic foams, fibrous, or granular materials is of great interest for a wide range of industrial applications. These materials are frequently used in the automotive and aeronautics industries and in the building trade. The determination of the properties of a medium using waves that have been reflected by or transmitted through the medium is a classical inverse scattering problem.⁵ Such problems are often approached by taking a physical model of the scattering process, generating a synthetic response for a number of assumed values for the parameters, and adjusting these parameters until a reasonable level of correspondence is attained between the synthetic response and the data observed. One important parameter which appears in theories of sound propagation in porous materials at low frequency range⁶ is the permeability k_0 . The permeability intervenes in

the description of the viscous coupling between the fluid and the structure. As such, in studies of acoustical properties of porous materials, it is extremely useful to be able to measure this parameter.

The permeability k_0 is related to the flow resistance.⁷⁻¹³ The flow resistance of porous material is defined as the ratio between the pressure difference across a sample and the velocity of flow of air through that sample; the flows being considered are steady and nonpulsating. This is quite analogous to the definition of electrical resistance as the ratio between voltage drop and current. The specific flow resistivity σ of a porous material is defined as the flow resistance per unit cube. The relation between viscous permeability k_0 and specific flow resistivity σ is given by $k_0 = \eta / \sigma$, where η is the fluid viscosity.

Many methods have been proposed in the past in the fluid mechanics field, developing instrumentation to measure accurately various properties of fluids.¹⁴ Systems for the

measurement of flow resistance are largely based on this technology, making use of techniques for measuring flow rates of fluids and pressure differences.

Among the various systems that have been developed for the measurement of flow resistance, a distinction can be made between direct and comparative methods. With direct methods, the pressure drop across a sample and the rate of air flow through the porous sample are determined separately and the flow resistance is computed as the ratio of the two quantities. One example of this type of system has been given by Morse *et al.*¹³ and Brown and Bolt.¹⁰ Air is drawn into a container after passing through a sample. Pressure differences are measured across the sample using a water nanometer, and air flows are obtained from the rate at which water siphons out of the container. Leonard¹¹ adapted an analytical beam balance to enable small pressure differences to be measured with considerably improved resolution. This technique, because of its simplicity and accuracy, is now widely used for the measurement of flow resistance. Bies and Hansen⁸ have improved upon the configuration of Morse *et al.*,¹³ using a “barocell” and digital nanometer to make precise measurements of pressure differences.

With comparative methods, a calibrated flow resistance is placed in series with the porous sample. The ratio of pressure drops across each element is the same as the ratio of the values of flow resistance, since the volumetric flow of air in the line is the constant. This method has been developed by Gemant,¹⁵ in which capillary tubes have been used as known flow resistances. Stinson and Daigle¹² have used a laminar flow element as a known flow resistance.

In this work, we present a simple acoustical method of measuring specific flow resistivity and thus the viscous permeability by measuring a diffusive wave transmitted by a slab of porous material in a guide (pipe). This method is based on a temporal model of the direct and inverse scattering problem for the diffusion of transient low frequency waves in a homogeneous isotropic slab of porous material having a rigid frame. This work was initially introduced by the authors of Ref. 6. The viscous and thermal losses of the medium are described by the Johnson *et al.*¹⁶ and Allard¹ model used in the time domain. Reflection and transmission scattering operators of a slab of porous material are derived, and thus the responses of the medium to an incident acoustic pulse are obtained.

The outline of this work is as follows. Section II recalls a time domain model and the basic equations of wave diffusion in porous material. Section III is devoted to the direct problem and to the general solution of the diffusive wave in porous media. Section IV contains the expressions of the reflection and transmission scattering operators in time domain. In Sec. V, the sensitivity of the porosity and the specific flow resistivity are discussed, showing the effect of each parameter on the transmitted wave by the porous slab. Section VI deals with the inverse problem and the appropriate procedure, based on the least-squares method, which is used to estimate the specific flow resistivity, and consequently, the viscous permeability. Finally in Sec. VII, experimental validation using low frequency acoustic measurement is discussed for air-saturated industrial plastic foams.

II. MODEL

In the acoustics of porous materials, one distinguishes two situations according to whether the frame is moving or not. In the first case, the dynamics of the waves due to the coupling between the solid skeleton and the fluid is well described by the Biot theory.¹⁷ In air-saturated porous media the structure is generally motionless and the waves propagate only in the fluid. This case is described by the model of equivalent fluid which is a particular case of the Biot model, in which the interactions between the fluid and the structure are taken into account in two frequency response factors: the dynamic tortuosity of the medium $\alpha(\omega)$ given by Johnson *et al.*¹⁶ and the dynamic compressibility of the fluid included in the porous material $\beta(\omega)$ given by Allard.¹ In the frequency domain, these factors multiply the density of the fluid and its compressibility, respectively, and represent the deviation from the behavior of the fluid in free space as the frequency changes.

A. Viscous domain (low frequency approximation)

The range of frequencies such that viscous skin thickness $\ell = (2\eta/\omega\rho_f)^{1/2}$ and thermal skin thickness $\ell' = (2\kappa/\rho_f C_p \omega)^{1/2}$ (ω is the angular frequency, η is the fluid viscosity, ρ_f is the fluid density, κ is the thermal conduction of the fluid, and C_p the specific thermal heat) are much larger than the radius of the pores r

$$\frac{\ell}{r} \gg 1$$

and

$$\frac{\ell'}{r} \gg 1 \quad (1)$$

is called the low frequency range. For these frequencies, the viscous forces are important everywhere in the fluid. At the same time, the compression-dilatation cycle in the porous material is slow enough to favor the thermal exchanges between fluid and structure. At the same time, the temperature of the frame is practically unchanged by the passage of the sound wave because of the high value of its specific heat and its high thermal conductivity: the frame acts as a thermostat. In this case the isothermal compressibility is directly applicable.^{1,6} Thermal losses are neglected for the sake of simplicity (there is no energy loss). Generally the viscous losses are the most important in the porous material and may represent approximatively 75% of the total losses.

In the time domain, the dynamic tortuosity and compressibility of the fluid included in the porous material act as operators and in the viscous domain (low frequency approximation) their expressions are given⁶ by

$$\begin{aligned} \tilde{\alpha}(t) &= \frac{\eta\phi}{\rho_f k_0} \bar{\sigma}_t^{-1}, \\ \tilde{\beta}(t) &= \gamma \delta(t), \end{aligned} \quad (2)$$

in these equations, $\delta(t)$ is the Dirac operator and $\bar{\sigma}_t^{-1}$ is the integral operator $\bar{\sigma}_t^{-1}g(t) = \int_0^t g(t')dt'$, γ is the adiabatic constant. The relevant physical parameter of the model is the

static permeability $k_0 = \eta / \sigma$, σ is the specific flow resistivity.

In this framework, the basic equations of our model can be written as

$$\rho_f \tilde{\alpha}(t) * \frac{\partial v_i}{\partial t} = -\nabla_i p,$$

$$\frac{\tilde{\beta}(t)}{K_a} * \frac{\partial p}{\partial t} = -\nabla \cdot v, \quad (3)$$

where $*$ denotes the time convolution operation, p is the acoustic pressure, v is the particle velocity, and K_a is the bulk modulus of the air. The first equation is the Euler equation, the second one is the constitutive equation.

Using Eqs. (2) and (3), we obtain along the x axis

$$\frac{\eta \phi}{k_0} v(x, t) = -\frac{\partial p(x, t)}{\partial x}, \quad (4)$$

$$\frac{\gamma}{K_a} \frac{\partial p(x, t)}{\partial t} = -\frac{\partial v(x, t)}{\partial x}. \quad (5)$$

The Euler equation is reduced to Darcy's law which expresses the balance between the driving force of the wave and the drag forces $\eta \phi v / k_0$ due to the flow resistance of the material.

The fields which are varying in time, the pressure, the acoustic velocity, etc., follow a diffusion equation⁶

$$\frac{\partial^2 p(x, t)}{\partial x^2} - D \frac{\partial p(x, t)}{\partial t} = 0, \quad (6)$$

with the diffusion constant

$$D = \frac{\eta \phi \gamma}{k_0 K_a}. \quad (7)$$

The diffusion constant D is a damping term due to the viscous and thermal effects which take place in the porous material. A quite similar result is given by Johnson.¹⁸ However, the adiabatic constant γ does not appear in Johnson's model in which the thermal expansion is neglected.

III. DIRECT PROBLEM

The direct scattering problem is that of determining the scattered field as well as the internal field that arises when a known incident field impinges on the porous material with known physical properties. To compute the solution of the direct problem one needs to know Green's function of the diffusive equation in the porous medium. In that case, the internal field is given by the time convolution of Green's function with the incident wave, and the reflected and transmitted fields are deduced from the internal field and the boundary conditions.

In this section some notation is introduced. The problem geometry is given in Fig. 1. A homogeneous porous material occupies region of $0 \leq x \leq L$. This medium is assumed to be isotropic and to have a rigid frame. A short sound pulse impinges normally on the medium from the left. It generates an acoustic pressure field $p(x, t)$ and an acoustic velocity field $v(x, t)$ within the material, which satisfy Eq (6) written also as

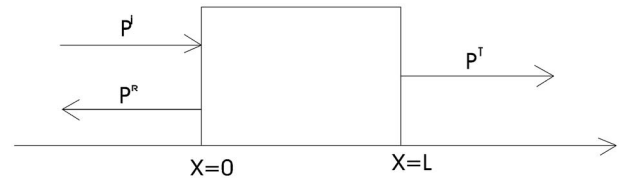


FIG. 1. Geometry of the problem.

$$\frac{\partial^2 p(x, t)}{\partial x^2} - DH(t) * \frac{\partial^2 p(x, t)}{\partial t^2} = 0, \quad (8)$$

where $H(t)$ is the Heaviside function:¹⁹ $H(t)=0$, for $t < 0$, $H(0)=1/2$ and $H(t)=1$, for $t > 0$.

To derive the reflection and transmission scattering operators, it is assumed that the pressure field and flow velocity are continuous at the material boundary,

$$p(0^+, t) = p(0^-, t), \quad p(L^-, t) = p(L^+, t),$$

$$v(0^-, t) = \phi v(0^+, t), \quad v(L^+, t) = \phi v(L^-, t), \quad (9)$$

where ϕ is the porosity of the medium and \pm superscript denotes the limit from left and right, respectively. Assumed initial conditions are

$$p(x, t)|_{t=0} = 0$$

and

$$\left. \frac{\partial p}{\partial t} \right|_{t=0} = 0, \quad (10)$$

which means that the medium is idle for $t=0$.

If the incident sound wave is generated in region $x \leq 0$, then the expression of the acoustic field in the region to the left of the material is the sum of the incident and reflected fields,

$$p_1(x, t) = p^i\left(t - \frac{x}{c_0}\right) + p^r\left(t + \frac{x}{c_0}\right), \quad x < 0, \quad (11)$$

here, $p_1(x, t)$ is the field in region $x < 0$ and p^i and p^r denote the incident and reflected fields, respectively. In addition, a transmitted field is produced in the region to the right of the material. This has the form

$$p_3(x, t) = p^t\left[t - \frac{(x-L)}{c_0}\right], \quad x > L. \quad (12)$$

[$p_3(x, t)$ is the field in region $x > L$ and p^t is the transmitted field.]

The incident and scattered fields are related by scattering operators (i.e., reflection and transmission operators) for the material. These are integral operators represented by

$$\begin{aligned} p^r(x, t) &= \int_0^t \tilde{R}(\tau) p^i\left(t - \tau + \frac{x}{c_0}\right) d\tau \\ &= \tilde{R}(t) * p^i(t) * \delta\left(t + \frac{x}{c_0}\right), \end{aligned} \quad (13)$$

$$p^i(x, t) = \int_0^t \tilde{T}(\tau) p^i \left[t - \tau - \frac{(x-L)}{c_0} \right] d\tau$$

$$= \tilde{T}(t) * p^i(t) * \delta \left[t - \frac{(x-L)}{c_0} \right]. \quad (14)$$

In Eqs. (13) and (14) functions \tilde{R} and \tilde{T} are the reflection and transmission kernels, respectively, for incidence from the left. Note that the lower limit of integration in Eq. (13), Eq. (14) is given as 0, which is equivalent to assuming that the incident wave front first impinges on the material at $t=0$. The operators \tilde{R} and \tilde{T} are independent of the incident field used in the scattering experiment and depend only on the properties of the materials.

The scattering operators given in Eqs. (13) and (14) are independent of the incident field used in scattering experiment and depend only on the properties of the materials. In the region $x \leq 0$, the field $p_1(x, t)$ is given by

$$p_1(x, t) = \left[\delta \left(t - \frac{x}{c_0} \right) + \tilde{R}(t) * \delta \left(t + \frac{x}{c_0} \right) \right] * p^i(t). \quad (15)$$

Equation (8) is solved by the Laplace transform method by taking into account the conditions (9) and (10). We note $P(x, z)$ the Laplace transform of $p(x, t)$ defined by

$$P(x, z) = \mathcal{L}[p(x, t)] = \int_0^\infty \exp(-zt) p(x, t) dt. \quad (16)$$

Using the following relations:

$$\mathcal{L}[\delta(t)] = 1$$

and

$$\mathcal{L}[H(t)] = \frac{1}{z}, \quad (17)$$

the Laplace transform of the diffusive equation [Eq. (8)] satisfying the initial conditions [Eq. (10)] becomes

$$\frac{\partial^2 P_2(x, z)}{\partial x^2} - Dz P_2(x, z) = 0, \quad (18)$$

where $P_2(x, z)$ is the Laplace transform of the acoustic pressure $p_2(x, t)$ inside the porous material for $0 \leq x \leq L$.

The Laplace transform of the field outside the materials is given by

$$P_1(x, z) = \left[\exp \left(-z \frac{x}{c_0} \right) + R(z) \exp \left(z \frac{x}{c_0} \right) \right] \varphi(z), \quad x \leq 0, \quad (19)$$

$$P_3(x, z) = T(z) \exp \left[-\frac{(x-L)}{c_0} z \right] \varphi(z), \quad x \geq L. \quad (20)$$

Here $P_1(x, z)$ and $P_3(x, z)$ are, respectively, the Laplace transform of the field at the left and the right sides of the material, $\varphi(z)$ denotes the Laplace transform of the incident field $p^i(t)$, and finally $R(z)$ and $T(z)$ are the Laplace transforms of the reflection and transmission kernels, respectively.

The Laplace transform of the continuous conditions (??) are written as

$$P_2(0^+, z) = P_1(0^-, z)$$

and

$$P_2(L^-, z) = P_3(L^+, z), \quad (21)$$

where $P_1(0^-, z)$ and $P_3(L^+, z)$ are the Laplace transforms of $p_1(x, t)$ and $p_3(x, t)$, respectively, given by

$$P_1(0^-, z) = [1 + R(z)] \varphi(z)$$

and

$$P_3(L^-, z) = T(z) \varphi(z), \quad (22)$$

from the Eqs. (18), (21), and (22), we deduce the expression of the field inside the material $P_2(x, z)$,

$$P_2(x, z) = \left\{ [1 + R(z)] \frac{\sinh[(L-x)\sqrt{Dz}]}{\sinh(L\sqrt{Dz})} + T(z) \frac{\sinh(x\sqrt{Dz})}{\sinh(L\sqrt{Dz})} \right\} \varphi(z), \quad (23)$$

where \sinh is the hyperbolic sine function.

The inverse Laplace transform of $\exp(-x\sqrt{Dz})$ gives the Green function of the medium,

$$G(x, t) = \mathcal{L}^{-1}[\exp(-x\sqrt{Dz})] = \frac{x\sqrt{D}}{2\sqrt{\pi}t^{3/2}} \exp\left(-\frac{x^2 D}{4t}\right). \quad (24)$$

The inverse Laplace transform of $P_2(x, z)$ gives the complete solution of the diffusive equation in time domain in the porous material taking into account the multiple reflections at the interfaces $x=0$ and $x=L$ (Appendix A).

$$p_2(x, t) = \sum_{n \geq 0} \{G[(2n+1)x, t] - G[(2n+1)(2L+x), t]\} * p_1(0, t) + \sum_{n \geq 0} \{G[(2n+1)(L-x), t] - G[(2n+1)(L+x), t]\} * p_3(L, t). \quad (25)$$

IV. REFLECTION AND TRANSMISSION SCATTERING OPERATORS

To derive the reflection and transmission coefficients, the boundary condition flow velocities at the interfaces $x=0$ and $x=L$ are needed.

The equation of the flow continuity at $x=0$ is written as

$$v_1(x, t) = \phi v_2(x, t), \quad (26)$$

where ϕ is the porosity of the medium.

The Euler equation is written in the regions (1) ($x \leq 0$) and (2) ($0 \leq x \leq L$) as

$$\rho_f \frac{\partial v_1(x, t)}{\partial t} \bigg|_{x=0} = - \frac{\partial p_1(x, t)}{\partial x} \bigg|_{x=0}, \quad x \leq 0, \quad (27)$$

$$\rho_f \tilde{\alpha}(t) * \frac{\partial v_2(x, t)}{\partial t} \bigg|_{x=0} = - \frac{\partial p_2(x, t)}{\partial x} \bigg|_{x=0}, \quad 0 \leq x \leq L, \quad (28)$$

where $v_1(x, t)$ and $v_2(x, t)$ are the acoustic velocity field in the regions (1) and (2), respectively. In the free space [region

(1)], the tortuosity operator is equal to 1. From Eqs. (26)–(28) it is easy to write

$$\tilde{\alpha}(t) * \left. \frac{\partial p_1(x,t)}{\partial x} \right|_{x=0} = \phi \left. \frac{\partial p_2(x,t)}{\partial x} \right|_{x=0}, \quad (29)$$

with

$$\left. \frac{\partial p_1(x,t)}{\partial x} \right|_{x=0} = \frac{1}{c_0} [-\delta(t) + \tilde{R}(t)] * \frac{\partial p^i(t)}{\partial t}. \quad (30)$$

The Laplace transform of Eq. (29) gives a relation between the reflection and transmission coefficients,

$$[R(z) - 1] \sinh(L\sqrt{Dz}) = \phi \rho_0 c_0 \frac{\sqrt{Dz}}{z\alpha(z)} \{T(z) - [1 + R(z)] \cosh(L\sqrt{Dz})\}, \quad (31)$$

where $\alpha(z)$ is the Laplace transform of $\tilde{\alpha}(t)$.

At the interface $x=L$, the continuity of the flow velocity leads to the relation

$$v_3(L^+, t) = \phi v_2(L^-, t). \quad (32)$$

At $x=L$, the Euler equation is written in the two regions (2) and (3) ($x \geq L$) as

$$\rho_f \tilde{\alpha}(t) * \left. \frac{\partial v_2(x,t)}{\partial t} \right|_{x=L^-} = - \left. \frac{\partial p_2(x,t)}{\partial x} \right|_{x=L^-} \\ \rho_f \left. \frac{\partial v_3(x,t)}{\partial t} \right|_{x=L^+} = - \left. \frac{\partial p_3(x,t)}{\partial x} \right|_{x=L^+}. \quad (33)$$

From Eqs. (32) and (33), we have

$$\tilde{\alpha}(t) * \left. \frac{\partial p_3(x,t)}{\partial x} \right|_{x=L^+} = \phi \left. \frac{\partial p_2(x,t)}{\partial x} \right|_{x=L^-}, \quad (34)$$

with

$$\left. \frac{\partial p_3(x,t)}{\partial x} \right|_{x=L^+} = - \frac{1}{c_0} \tilde{T}(t) * \left. \frac{\partial p^i}{\partial t} \right|_{t=L/c_0}, \quad (35)$$

the Laplace transform of Eq. (34) gives

$$T(z) \sinh(L\sqrt{Dz}) = \phi \rho_0 c_0 \frac{\sqrt{Dz}}{z\alpha(z)} [1 + R(z) - T(z) \cosh(L\sqrt{Dz})]. \quad (36)$$

By putting

$$B = \frac{\phi \rho_0 c_0 \sqrt{D}}{z\alpha(z)} = \sqrt{\frac{\rho_0^3 \phi \gamma}{\eta k_0}}. \quad (37)$$

The reflection and transmission coefficients are the solution of the system of equations [Eqs. (31) and (36)],

$$R(z) [\sinh(L\sqrt{Dz}) + B\sqrt{z} \cosh(L\sqrt{Dz})] - B\sqrt{z} T(z) \\ = \sinh(L\sqrt{Dz}) - B\sqrt{z} \cosh(L\sqrt{Dz}), \\ -R(z) B\sqrt{z} + T(z) [\sinh(L\sqrt{Dz}) + B\sqrt{z} \cosh(L\sqrt{Dz})] = B\sqrt{z}. \quad (38)$$

$R(z)$ and $T(z)$ are given by

$$R(z) = \frac{(1 - B^2 z) \sinh(L\sqrt{Dz})}{2B\sqrt{z} \cosh(L\sqrt{Dz}) + (1 + B^2 z) \sinh(L\sqrt{Dz})}, \quad (39)$$

$$T(z) = \frac{2B\sqrt{z}}{2B\sqrt{z} \cosh(L\sqrt{Dz}) + (1 + B^2 z) \sinh(L\sqrt{Dz})}. \quad (40)$$

The development of these expressions in exponential series (Appendix B) leads to the reflection and transmission coefficients,

$$R(z) = \frac{1 - B\sqrt{z}}{1 + B\sqrt{z}} \sum_{n \geq 0} \left(\frac{1 - B\sqrt{z}}{1 + B\sqrt{z}} \right)^{2n} \{ \exp(-2nL\sqrt{Dz}) \\ - \exp[-2(n+1)L\sqrt{Dz}] \}, \quad (41)$$

$$T(z) = \frac{4B\sqrt{z}}{(1 + B\sqrt{z})^2} \sum_{n \geq 0} \left(\frac{1 - B\sqrt{z}}{1 + B\sqrt{z}} \right)^{2n} \\ \times \exp[-(2n+1)L\sqrt{Dz}]. \quad (42)$$

These expressions take into account the multiple reflections in the material.

In most cases, in porous materials saturated by air, the multiply reflection effects are negligible because of the high attenuation of sound waves in these media. So, by taking into account only the first reflections at the interfaces $x=0$ and $x=L$, the transmission coefficient in the material becomes

$$T(z) = \frac{4B\sqrt{z}}{(1 + B\sqrt{z})^2} \exp(-L\sqrt{Dz}). \quad (43)$$

The transmission scattering operator is calculated by taking the inverse Laplace transform of the transmission coefficient,

$$\tilde{T}(t) = \mathcal{L}^{-1} \left[\frac{4B\sqrt{z}}{(1 + B\sqrt{z})^2} \right] * G(L, t), \quad (44)$$

$G(L, t)$ is the Green function of the porous material given by the relation (24).

We infer²⁰ that

$$\mathcal{L}^{-1} \left[\frac{4B\sqrt{z}}{(1 + B\sqrt{z})^2} \right] = D_1(t) = \frac{2}{B\sqrt{\pi}} \frac{1}{t^{3/2}} \int_0^\infty \left(\frac{u^2}{4t} - 1 \right) u \\ \times \exp\left(-\frac{u^2}{4t}\right) \exp\left(-\frac{u}{B}\right) du, \\ = \frac{2B}{\sqrt{\pi}} \frac{1}{t^{3/2}} \int_0^\infty \left(\frac{B^2 y^2}{4t} - 1 \right) y \exp\left(-\frac{B^2 y^2}{4t}\right) \exp(-y) dy.$$

The transmission scattering operator is given by

$$\tilde{T}(t) = D_1(t) * G(L, t). \quad (45)$$

The time domain expression of the transmission scattering operator $\tilde{T}(t)$ is important for the simulation of transient transmitted wave directly in time domain. The convolution of $\tilde{T}(t)$ with the incident signal [Eq. (14)] gives us the transmitted signal in the time domain.

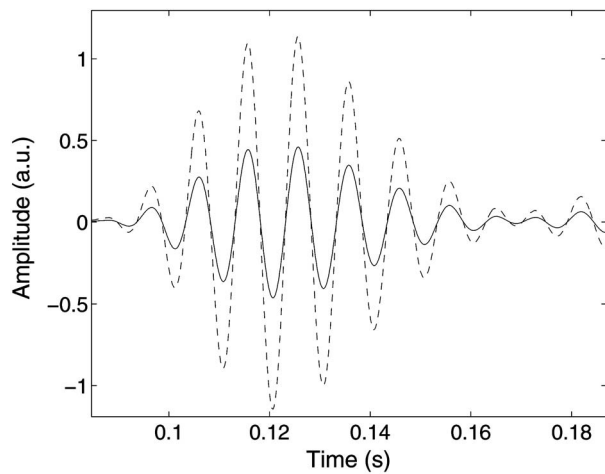


FIG. 2. Incident signal (dashed line) and simulated transmitted signal (solid line).

V. ACOUSTIC PARAMETER SENSITIVITY

In this section, numerical simulations of waves transmitted by a slab of porous material are run by varying the independent geometrical parameters of a porous medium described acoustically using the theory developed in the previous section. 50% variation is applied to the governing parameters (flow resistivity σ and porosity ϕ). The numerical values chosen for the physical parameters correspond to quite common acoustic materials, as follows: thickness $L=4$ cm, porosity $\phi=0.9$ and flow resistivity $\sigma=30\,000\text{ N m}^{-4}\text{ s}$, and radius of the pore $r=70\text{ }\mu\text{m}$. The condition of viscous domain (low frequency approximation) is verified if the frequencies of the incident signal spectrum are much smaller than the characteristic frequency which verify Eq. (1). For this porous sample the characteristic frequency is equal to 1 kHz.

A first numerical simulation is produced. The incident signal used in the simulation is given in Fig. 2 (dashed line). The result of the simulation (transmitted wave) is a signal as shown in the same figure (Fig. 2) in solid line. Amplitude is given by an arbitrary unit and the point number given in the abscissa is proportional to time. The spectra of the incident and transmitted signals are given in Fig. 3. From Fig. 2, we can see that there is no delay between the incident and simulated transmitted signals, the two waves have the same arrival time. The transmitted wave is just attenuated with no significant dispersion comparing to the incident signal, the two signals have the same spectral bandwidth (Fig. 3). These results are in adequacy with the theory of viscous domain (low frequency range) developed in previous sections, in which the propagation equation is reduced to a diffusive equation [Eq. (6)]. Generally, the inertial effects in porous materials described by the tortuosity⁵ (α_∞) are the essential cause of propagation, with wave front velocity $c=c_0/\sqrt{\alpha_\infty}$ (c_0 is the wave velocity in free fluid). In the low frequency domain, the inertial effects are negligible near the viscous exchange between fluid and structure, the tortuosity does not appear in the model and thus there is no propagation in the porous material.

Figure 4 shows the results obtained after reducing flow

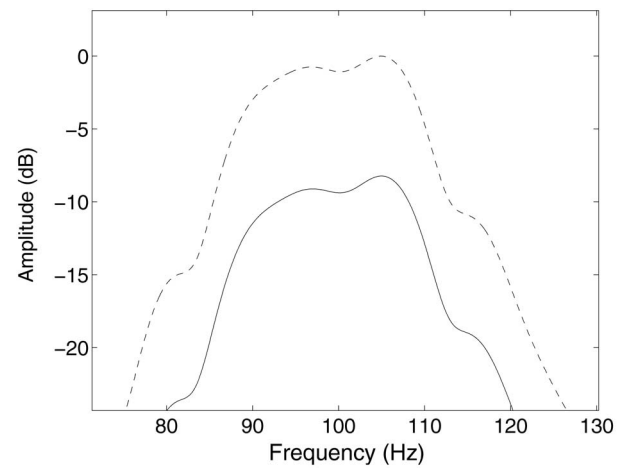


FIG. 3. Spectrum of incident signal (dashed line) and spectrum of transmitted signal (solid line).

resistivity by 50% of its initial value. The first signal (dashed line) corresponds to the simulated transmitted signal for $\sigma=30\,000\text{ N m}^{-4}\text{ s}$ and the second one (solid line) to $\sigma=15\,000\text{ N m}^{-4}\text{ s}$. The values of the other parameters have been kept constant ($L=4$ cm and porosity $\phi=0.9$). The sensitivity of the flow resistivity in transmitted mode can be seen for a 50% change. By reducing flow resistivity, the amplitude of the transmitted wave increases by 50% of its initial value. This result can be explained by the fact that when flow resistivity decreases (permeability increases), the losses due to the viscous effects become less important in the porous material, and thus the amplitude of the transmitted wave is less attenuated.

By reducing the porosity by 50% of its initial value, no important change appears in the transmitted wave (Fig. 5). We can conclude that there is no significant sensitivity to porosity in transmission mode.

From this study, we can gain an insight into the sensitivity of each physical parameter used in this theory. It seems that the flow resistivity is the most important parameter in the description of losses in the viscous domain (low fre-

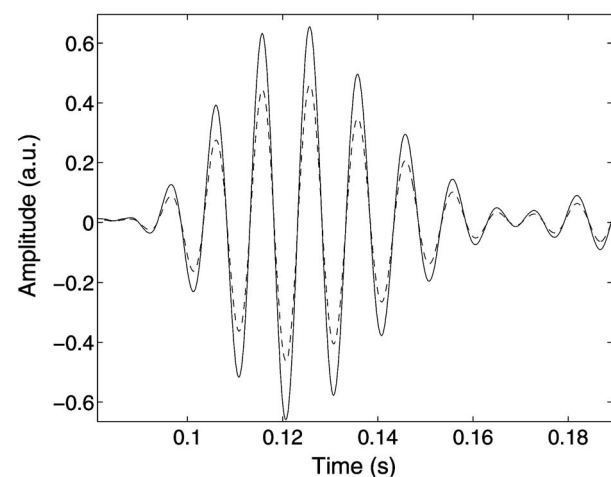


FIG. 4. Comparison between simulated transmitted signals corresponding to $\sigma=30\,000\text{ N m}^{-4}\text{ s}$ (dashed line) and $\sigma=15\,000\text{ N m}^{-4}\text{ s}$ (solid line).

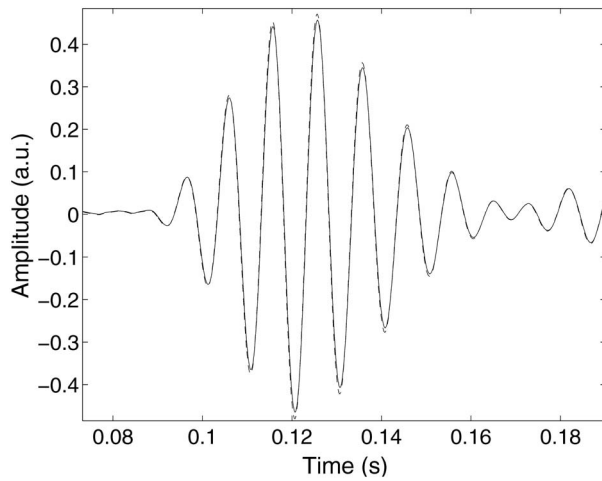


FIG. 5. Comparison between simulated transmitted signals corresponding to $\phi=0.45$ (dashed line) and $\phi=0.9$ (solid line).

quency range). We will try to measure this parameter in the next sections by solving the inverse problem using experimental data of transmitted waves.

VI. INVERSE PROBLEM

The diffusion of acoustic waves in a slab of porous material in the viscous domain is characterized by two parameters, namely, porosity ϕ and flow resistivity σ , the values of which are crucial for the behavior of sound waves in such materials. It is of some importance to work out new experimental methods and efficient tools for their estimation. The basic inverse problem associated with the slab may be stated as follows: from measurement of the signals transmitted and/or reflected outside the slab, find the values of the medium's parameters. In this paper, only the transmitted waves are studied. The study of the sensitivity of the porosity shows that this parameter cannot be estimated in transmission mode because of its weak sensitivity. Porosity was estimated in reflection in our previous studies^{21–24} in the asymptotic domain (high frequency range), by solving the inverse problem at normal^{22,24} and oblique incidence^{21,23} for plastic foams and air-saturated random packings of beads, by measuring reflected waves for different incident angles. It has been shown in the previous section that the flow resistivity has a significant sensitivity on transmitted waves. We will try to determine σ by solving the inverse problem for waves transmitted by the slab of porous material. The inverse problem is to find value for parameter σ which minimize the function

$$U(\sigma) = \int_0^t [p_{\text{exp}}^t(x, t) - p^t(x, t)]^2 dt,$$

where $p_{\text{exp}}^t(x, t)$ is the experimentally determined transmitted signal and $p^t(x, t)$ is the transmitted wave predicted from Eq. (14). However, the analytical method of solving the inverse problem using the conventional least-squares method is tedious. In our case, a numerical solution of the least-squares method can be found which minimizes $U(\sigma)$ defined by

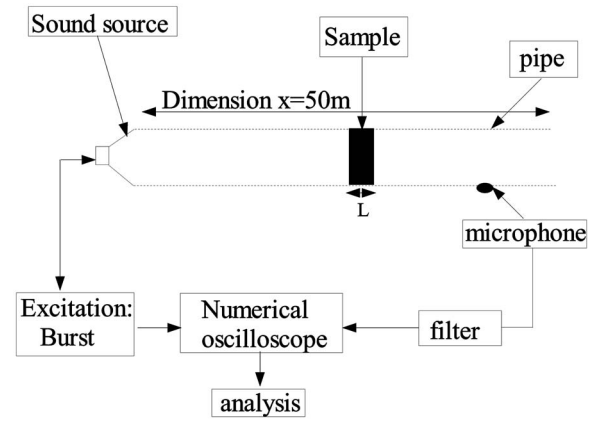


FIG. 6. Experimental setup of acoustic measurements.

$$U(\sigma) = \sum_{i=1}^{i=N} [p_{\text{exp}}^t(x, t_i) - p^t(x, t_i)]^2, \quad (46)$$

where $p_{\text{exp}}^t(x, t_i)_{i=1,2,\dots,N}$ represents the discrete set of values of the experimental transmitted signal and $p^t(x, t_i)_{i=1,2,\dots,N}$ is the discrete set of values of the simulated transmitted signal. The inverse problem is solved numerically by the least-squares method. The next section discusses solution of the inverse problem based on experimental transmitted data.

VII. ACOUSTIC MEASUREMENTS

In application of our model, some numerical simulations are compared with experimental results. To verify the condition of low frequency range for air-saturated plastic foams having pores radius between 40 and 100 μm , the frequency component of the experimental signals must be very small compared to 1 kHz [Eq. (1)]. Experiments are performed in a guide (pipe), having a diameter of 5 cm and of length 50 m. This length has been chosen for the propagation of transient signals at low frequency. It is not important to keep the pipe straight, it can be rolled in order to save space without perturbations on experimental signals (the cutoff frequency of the tube $f_c \sim 4$ kHz).

A sound source driver unit “Brand” constituted by loudspeaker Realistic 40-9000 is used. Bursts are provided by synthesized function generator Stanford Research Systems model DS345 30 MHz. The signals are amplified and filtered using model SR 650 dual channel filter, Stanford Research Systems. The signals (incident and transmitted) are measured using the same microphone (Bruel & Kjaer, 4190) in the same position in the tube. The incident signal is measured without porous sample, however, the transmitted signal is measured with the porous sample; the experimental setup is shown in Fig. 6.

Consider a cylindrical sample of plastic foam M1 of diameter of 5 cm and thickness of 2.5 cm. Sample M1 was characterized using classical methods^{8,10–12} given the following physical parameters: $\phi=0.9\pm0.01$, $\sigma=38\,000\pm6000$ N m⁻⁴ s, and $k_0=(0.48\pm0.09)\times10^{-9}$ m².

Figure 7 shows the experimental incident signal (solid line) generated by the loudspeaker in the frequency bandwidth of 25–60 Hz, and the experimental transmitted signal

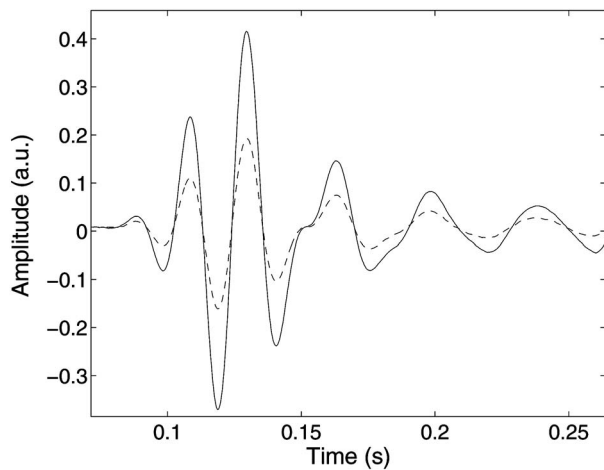


FIG. 7. Experimental incident signal (solid line) and experimental transmitted signal (dashed line).

(dashed line). Figure 8 shows the spectra of the two signals. From the spectra of the two signals, the reader can see that they have practically the same bandwidth which means that there is no dispersion. After solving the inverse problem numerically for the flow resistivity, we find the following optimized value: $\sigma = 39\,500 \pm 2000 \text{ N m}^{-4} \text{ s}$, which is equivalent to the optimized value of the viscous permeability $k_0 = (0.46 \pm 0.03) \times 10^{-9} \text{ m}^2$. We present in Fig. 9 the variation of the minimization function U given in Eq. (46) with the flow resistivity σ . In Fig. 10, we show a comparison between an experimental transmitted signal and simulated transmitted signal for the optimized value of the flow resistivity. The difference between the two curves is slight, which leads us to conclude that the optimized value of the flow resistivity (and thus for the viscous permeability) is correct.

The inverse problem has been solved for the sample M1 in the frequency bandwidth of 85–115 Hz; we obtain the following optimized value of the flow resistivity: $\sigma = 40\,500 \pm 2000 \text{ N m}^{-4} \text{ s}$, its equivalent value of the viscous permeability is $k_0 = (0.45 \pm 0.03) \times 10^{-9} \text{ m}^2$. Here, again, the correlation of theoretical prediction and experimental data is good. This study has been carried on, in the frequency band-

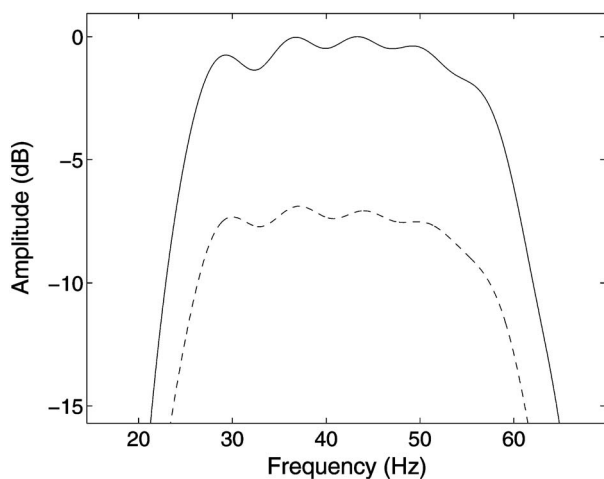


FIG. 8. Spectrum of experimental incident signal (solid line) and of experimental transmitted signal (dashed line).

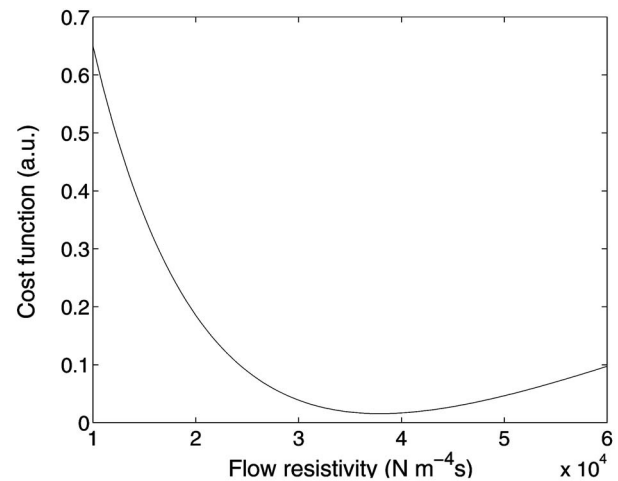


FIG. 9. Variation of the minimization function U with flow resistivity σ .

width of 130–190 Hz and have also given good results. It can be seen that for the different frequency bandwidths of the experimental incident signals, the optimized values obtained using this method are close to those produced using classical methods.^{8,10–12}

Let us consider another sample M2 more resistive, of diameter of 5 cm and thickness of 4.15 cm. Sample M2 was characterized using classical methods^{8,10–12} given the following physical parameters: $\phi = 0.85 \pm 0.01$, $\sigma = 80\,000 \pm 6000 \text{ N m}^{-4} \text{ s}$, and $k_0 = (0.23 \pm 0.09) \times 10^{-9} \text{ m}^2$. Different frequency bandwidths have been investigated between 50 and 250 Hz. By solving the inverse problem for the flow resistivity and minimizing the cost function U given by Eq. (46), the results of the inverse problem give $\sigma_1 = 79\,500 \pm 4000 \text{ N m}^{-4} \text{ s}$, $\sigma_2 = 80\,500 \pm 4000 \text{ N m}^{-4} \text{ s}$, and $\sigma_3 = 83\,000 \pm 4000 \text{ N m}^{-4} \text{ s}$. The reader can see the slight difference between the optimized values of the flow resistivity obtained with this method and the other classical method.^{8,10–12} The agreement between experiment and theory is good, which leads us to conclude that this method based

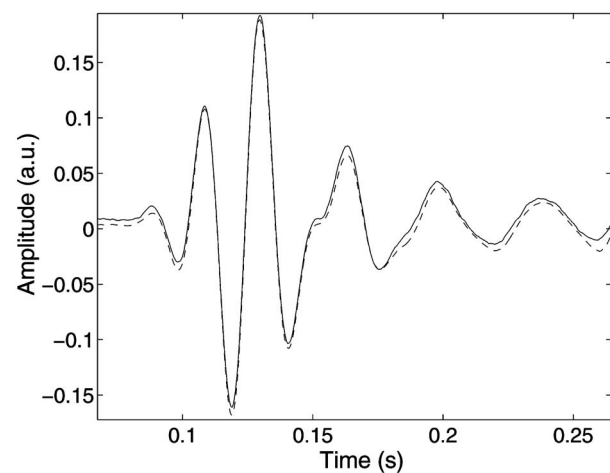


FIG. 10. Comparison between experimental transmitted signal (dashed line) and simulated transmitted signal (solid line) for the sample M1.

on solving the inverse problem is appropriate for estimating the flow resistivity and viscous permeability of porous materials with rigid frame.

VIII. CONCLUSION

In this article, an inverse scattering estimate of the flow resistivity and viscous permeability was given by solving the inverse problem for waves transmitted by slab of air-saturated porous material. The inverse problem is solved numerically by the least-squares method. The reconstructed values of flow resistivity and viscous permeability are close to those using classical methods. This method is an alternative to the usual methods^{8,10-12} that involves the use of techniques for measuring the flow rate of fluids and pressure differences.

The direct problem is based on the diffusion equation in the time domain in a slab of porous material in the viscous domain (low frequency range). Interaction of the sound pulse with the fluid-saturated porous material was described by a time domain equivalent fluid model.

The sensitivity analysis of ϕ and σ was studied in this paper, showing the importance of the values of these parameters in the transmitted wave. This study has demonstrated that flow resistivity is much more sensitive than porosity to transmission; the effect of the porosity in transmission is negligible as it has been observed in the asymptotic domain (high frequency range).⁵

We hope, in the future, to extend this method to porous media with elastic frame, such as cancellous bone saturated with viscous fluid, in order to estimate other parameters which play an important role in the acoustic propagation. The advantage of the data concept using diffusive wave is its simple analysis, and similar to the propagative wave concept which, however, is more complicated. The diffusive wave at low frequency is not subjected to dispersion but is simply attenuated, its frequency and temporal bandwidth are the same as the incident signal, and its experimental detection is easy for resistive media compared to propagative transmitted wave in the asymptotic domain (high frequency range).

APPENDIX A: EXPRESSION OF THE ACOUSTIC FIELD INSIDE THE POROUS MATERIAL

The expression of the acoustic field inside the porous material taking into account the multiple reflection at the interfaces $x=0$ and $x=L$ is given from Eq. (23),

$$P_2(x, z) = P_1(0^-, z) \frac{\sinh(\varepsilon\sqrt{Dz})}{\sinh(\xi\sqrt{Dz})} + P_3(L^+, z) \frac{\sinh(\theta\sqrt{Dz})}{\sinh(\xi\sqrt{Dz})},$$

with $\varepsilon=L-x$, $\xi=L$, and $\theta=x$ by the following development in series:

$$\begin{aligned} \frac{\sinh(\varepsilon\sqrt{Dz})}{\sinh(\xi\sqrt{Dz})} &= \frac{\exp(\varepsilon\sqrt{Dz}) - \exp(-\varepsilon\sqrt{Dz})}{\exp(\xi\sqrt{Dz}) - \exp(-\xi\sqrt{Dz})} \\ &= \frac{\exp(\varepsilon\sqrt{Dz}) - \exp(-\varepsilon\sqrt{Dz})}{\exp(\xi\sqrt{Dz})[1 - \exp(-2\xi\sqrt{Dz})]} \\ &= \frac{\exp(\varepsilon\sqrt{Dz}) - \exp(-\varepsilon\sqrt{Dz})}{\exp(\xi\sqrt{Dz})} \sum_{n \geq 0} \end{aligned}$$

$$\begin{aligned} &\times \exp(-2n\xi\sqrt{Dz}) = [\exp(\varepsilon\sqrt{Dz}) \\ &- \exp(-\varepsilon\sqrt{Dz})] \sum_{n \geq 0} \exp[-(2n+1)\xi\sqrt{Dz}] \\ &= \sum_{n \geq 0} (\exp\{-(2n+1)\xi - \varepsilon\}\sqrt{Dz}\} \\ &- \exp\{-(2n+1)\xi + \varepsilon\}\sqrt{Dz}\}), \end{aligned}$$

and the inverse Laplace transform of $P_2(x, z)$,

$$\begin{aligned} p_2(x, t) = \mathcal{L}^{-1} P_2(x, z) &= p_1(0, t) * \mathcal{L}^{-1} \left[\frac{\sinh(\varepsilon\sqrt{Dz})}{\sinh(\xi\sqrt{Dz})} \right] \\ &+ p_3(L, t) * \mathcal{L}^{-1} \left[\frac{\sinh(\theta\sqrt{Dz})}{\sinh(\xi\sqrt{Dz})} \right], \end{aligned}$$

where

$$\mathcal{L}^{-1} \left[\frac{\sinh(\varepsilon\sqrt{Dz})}{\sinh(\xi\sqrt{Dz})} \right] = \sum_{n \geq 0} \{G[(2n+1)\xi - \varepsilon, t] - G[(2n+1)\xi + \varepsilon, t]\}$$

and

$$G(x, t) = \mathcal{L}^{-1}[\exp(-x\sqrt{Dz})]$$

are given by Eq. (24).

The field $p_2(x, t)$ inside the porous medium is given then by

$$\begin{aligned} p_2(x, t) &= p_1(0, t) * \sum_{n \geq 0} \{G[(2n+1)\xi - \varepsilon, t] - G[(2n+1)\xi \\ &+ \varepsilon, t]\} + p_3(L, t) * \sum_{n \geq 0} \{G[(2n+1)\xi - \theta, t] \\ &- G[(2n+1)\xi + \theta, t]\}. \end{aligned}$$

By substituting ε , ξ , and θ by their values, we find the expression (25).

APPENDIX B: EXPRESSION OF THE REFLECTION AND TRANSMISSION COEFFICIENTS

After developing [in Eq. (39)] the hyperbolic sine and cosine functions in exponential series, we obtain the following expressions of the reflection coefficient $R(z)$:

$$\begin{aligned} R(z) &= \frac{(1 - B^2z)[\exp(L\sqrt{Dz}) - \exp(-L\sqrt{Dz})]}{(1 + B\sqrt{z})^2 \exp(L\sqrt{Dz}) - (1 - B\sqrt{z})^2 \exp(-L\sqrt{Dz})}, \\ &= \frac{1 - B\sqrt{z}}{1 + B\sqrt{z}} [1 - \exp(-2L\sqrt{Dz})] \frac{1}{1 - \left(\frac{1 - B\sqrt{z}}{1 + B\sqrt{z}}\right)^2 \exp(-2L\sqrt{Dz})}, \\ &= \frac{1 - B\sqrt{z}}{1 + B\sqrt{z}} [1 - \exp(-2L\sqrt{Dz})] \sum_{n \geq 0} \left(\frac{1 - B\sqrt{z}}{1 + B\sqrt{z}}\right)^{2n} \\ &\quad \times \exp(-2nL\sqrt{Dz}). \end{aligned}$$

Finally, we obtain the expression of the reflection coefficient taking into account the n -multiple reflections in the material,

$$R(z) = \frac{1 - B\sqrt{z}}{1 + B\sqrt{z}} \sum_{n \geq 0} \left(\frac{1 - B\sqrt{z}}{1 + B\sqrt{z}} \right)^{2n} \{ \exp(-2nL\sqrt{Dz}) - \exp[-2(n+1)L\sqrt{Dz}] \}.$$

In the same manner, the expression of the transmission coefficient $T(z)$ [Eq. (40)] can be written as

$$\begin{aligned} T(z) &= \frac{4B\sqrt{z}}{(1 + B\sqrt{z})^2 \exp(L\sqrt{Dz}) - (1 - B\sqrt{z})^2 \exp(-L\sqrt{Dz})} \\ &= \frac{4B\sqrt{z}}{(1 + B\sqrt{z})^2} \exp(-L\sqrt{Dz}) \frac{1}{1 - \left(\frac{1 - B\sqrt{z}}{1 + B\sqrt{z}} \right)^2 \exp(-2L\sqrt{Dz})}. \end{aligned}$$

The final expression of the transmission coefficient is given by

$$T(z) = \frac{4B\sqrt{z}}{(1 + B\sqrt{z})^2} \sum_{n \geq 0} \left(\frac{1 - B\sqrt{z}}{1 + B\sqrt{z}} \right)^{2n} \exp[-(2n + 1)L\sqrt{Dz}].$$

¹J. F. Allard, *Propagation of Sound in Porous Media: Modeling Sound Absorbing Materials* (Chapman and Hall, London, 1993).

²K. Attenborough, J. Acoust. Soc. Am. **81**, 93 (1987).

³K. Attenborough, J. Acoust. Soc. Am. **73**, 785 (1983).

⁴K. Attenborough, Acta. Acust. Acust. **1**, 213 (1993).

⁵Z. E. A. Fella, M. Fella, W. Lauriks, and C. Depollier, J. Acoust. Soc. Am. **113**, 61 (2003).

⁶Z. E. A. Fella and C. Depollier, J. Acoust. Soc. Am. **107**, 683 (2000).

⁷M. E. Delany and E. N. Bazley, Appl. Acoust. **3**, 105 (1970).

⁸D. A. Bies and C. H. Hansen, Appl. Acoust. **13**, 357 (1980).

⁹T. F. W. Embleton, J. E. Piercy, and G. A. Daigle, J. Acoust. Soc. Am. **74**, 1239 (1983).

¹⁰R. L. Brown and R. H. Bolt, J. Acoust. Soc. Am. **13**, 337 (1942).

¹¹R. W. Leonard, J. Acoust. Soc. Am. **17**, 240 (1946).

¹²M. R. Stinson and G. A. Daigle, J. Acoust. Soc. Am. **83**, 2422 (1988).

¹³P. M. Morse, R. H. Bolt, and R. L. Brown, J. Acoust. Soc. Am. **12**, 475 (1941) (Abstract).

¹⁴*Fluid Mechanics Measurements*, edited by Richard J. Goldstein (Hemisphere, New York, 1983).

¹⁵A. Gemant, J. Appl. Phys. **12**, 725 (1941).

¹⁶D. L. Johnson, J. Koplik, and R. Dashen, J. Fluid Mech. **176**, 379 (1987).

¹⁷M. A. Biot, J. Acoust. Soc. Am. **28**, 168 (1956).

¹⁸D. J. Johnson, *Proceeding of the International School of Physics Enrico Fermi, Course XCIII*, edited by D. Sette (North Holland, Amsterdam, 1986), pp. 255–290.

¹⁹E. W. Weisstein, *Concise Encyclopedia of Mathematics* (Chapman and Hall, Boca Raton, 1999).

²⁰I. S. Gradshteyn and I. M. Ryzhik, *Table of Integrals, Series, and Products*, 4th ed. (Academic, New York, 1965).

²¹Z. E. A. Fella, S. Berger, W. Lauriks, C. Depollier, C. Aristegui, and J. Y. Chapelon, J. Acoust. Soc. Am. **113**, 2424 (2003).

²²Z. E. A. Fella, C. Depollier, S. Berger, W. Lauriks, P. Trompette, and J. Y. Chapelon, J. Acoust. Soc. Am. **114**, 2561 (2003).

²³Z. E. A. Fella, F. G. Mitri, C. Depollier, S. Berger, W. Lauriks, and J. Y. Chapelon, J. Appl. Phys. **94**, 7914 (2003).

²⁴Z. E. A. Fella, S. Berger, W. Lauriks, C. Depollier, and M. Fella, J. Appl. Phys. **93**, 296 (2003).